有机化学 DOI: 10.6023/cjoc202409031 研究论文
Chinese Journal of Organic Chemistry ARTICLE

一种具有非稠合氮杂环端基的 A-D-A 型分子的合成及性能研究

刘文睿[a] 音正春[b] 叶世棋[a] 徐智伟[a] 陈 龙[a] 王官武*[,a,b,c]

([a]中国科学技术大学化学系 合肥 230026)

([b]安徽师范大学化学与材料科学学院 功能分子固体教育部重点实验室 分子基材料安徽省重点实验室 安徽芜湖 241002)

([c]兰州大学应用有机化学国家重点实验室 兰州 730000)

摘要 在具有新型非稠合氮杂环端基苯基吡唑啉酮的苯环上进行了以氯为代表的端基修饰, 获得了一系列受体-供体-受体(A-D-A)型分子. 这种非稠合氮杂环端基分子苯基吡唑啉酮与经典的端基分子丙二腈茚二酮类相比, 具有合成步骤简单、成本低廉、环境友好等优势. 对合成的具有非稠合氮杂环端基的 A-D-A 型分子进行了相关性质的探究, 通过理论计算对合成的 A-D-A 型分子性质进行了预测, 并进行了紫外可见吸收、循环伏安曲线、X 射线衍射和电子迁移率等测试, 表明了合成的 A-D-A 型分子的紫外可见吸收集中于波长 500～700 nm 区间, 具有接近 1.7 eV 的中等带隙. 同时通过对比探究了端基氯代对分子性质的影响, 这种非稠合氮杂环端基的受体分子被证明具有作为钙钛矿太阳能电池器件中的界面修饰层来修饰活性层的应用潜力.

关键词 A-D-A 型分子; n 型半导体; 非稠合端基; 中等带隙

Synthesis and Properties of Novel A-D-A Type Molecules with Non-Fused Azacyclic End Groups

Liu, Wenrui[a] Yin, Zhengchun [b] Ye, Shiqi [a] Xu, Zhiwei[a]

Chen, Long[a] Wang, Guanwu*[,a,b,c]

([a] *Department of Chemistry, University of Science and Technology of China, Hefei 230026*)

([b] *Key Laboratory of Functional Molecular Solids, Ministry of Education, Anhui Laboratory of Molecule-Based Materials, and School of Chemistry and Materials Science, Anhui Normal University, Wuhu, Anhui 241002*)

([c] *State Key Laboratory of Applied Organic Chemistry, Lanzhou University, Lanzhou 730000*)

Abstract Acceptor-donor-acceptor (A-D-A) type molecules, of which the novel non-fused azacyclic end-group pyrazolinones were modified with chlorine substitution on the phenyl ring, were synthesized. The non-fused azacyclic end-group pyrazolinones have the advantages of simple synthesis steps, low cost and environmental friendliness, compared to the classical end-group dicyanomethyleneindianone. The properties of the synthesized A-D-A type molecules with non-fused azacyclic end groups were characterized by theoretical calculation, UV-vis absorption, cyclic voltammetry, X-ray diffraction and space charge limited current. It is shown that the strong UV-vis absorptions of the synthesized A-D-A type molecules are located in the wavelength range of 500～700 nm, with a moderate band gap of nearly 1.7 eV. At the same time, the influence of end-group chlorination on the properties of A-D-A type molecules was compared and explored. It is proven that this kind of A-D-A type molecule with non-fused azacyclic end groups has the potential to be applied as interfacial modified layer of the active layer in perovskite solar cell devices.

Keywords A-D-A type molecule; n-type semiconductor; Non-fused end groups; Medium bandgap

1 Introduction

n-Type organic semiconductor materials have attracted much attention in the field of solar cells due to their light weight, flexibility, adjustability and solution processability.[1-8] In terms of n-type organic semiconductor materials, small molecular materials with acceptor-donor-acceptor (A-D-A) structures have emerged as a prevailing class,

* Corresponding author. E-mail: gwang@ustc.edu.cn

Received September 23, 2024; revised October 23, 2024; published online October 29, 2024.

Project supported by the National Natural Science Foundation of China (No. 22271271).

国家自然科学基金(No. 22271271)资助项目.

where A is electron-deficient moiety, and D is an electron-rich moiety.[9-15] Molecules with A-D-A structures are usually composed of fused aromatic cores, bulky alkyl side chains and highly electron-deficient end groups, and have been widely known and studied due to their many advantages, including high flexibility in chemical structure modification, energy level tunability and strong light absorption in the visible and near-infrared (NIR) regions.[16-19]

A representative A-D-A type molecule Y6 with highly electron-deficient end-group IC2F (Figure 1a) was reported, and the corresponding solar cell devices achieved an impressive power conversion efficiency (PCE) of 15.7%.[11] Subsequently, researchers manipulated the structures of A-D-A type molecules by introducing linear or branched alkyl side chains of different lengths, and modifying the aromatic cores and end groups of the molecules. However, the end group is mostly limited to the fused 1,1-dicyanomethylene-3-indanone (IC) unit and its derivatives.[20-28] Therefore, end-group engineering and subsequent interfacial modification engineering have become good strategies to overcome these limitations.[29-41] Moreover, A-D-A type molecules have been successfully applied as interfacial modified layers (IMLs) of perovskite cell devices, resulting in significant improvements in device performance.[42-47]

Guo, Li and coworkers reported a hydroxylated nonfullerene acceptor IT-DOH with A-D-A structure to modify the interface between the perovskite and the electron transport layer (ETL), and increased PCE of inverted perovskite solar cells from 19.08% to 22.09%.[25] Similarly, Ge and coworkers synthesized a series of A-D-A molecules (Y-H, Y-F, and Y-Cl) to optimize the properties of the perovskite/ETL interface. When these modifier layers were applied to enhance the efficiency of $Cs_{0.05}(FA_{0.95}MA_{0.05})_{0.95}PbI_{2.64}Br_{0.36}$-based device, a champion PCE exceeding 24% was achieved in the Y-F-based FAMA device.[43] Moreover, Zhang, Fang and coworkers designed a novel A-D-A material (IDIS-Th) with sulfonyl groups as interfacial modification layer. The IDIS-Th-containing PSC device achieved a high efficiency of over 20%, with a heightened V_{OC} of 1.116 V, J_{SC} of 22.67 mA cm^{-2} and fill factor (FF) of 79.1%.[46]

Despite the above progress made in the synthesis of A-D-A type molecules with IC end groups, the synthesis and purification of fused end-group IC units and their derivatives are still not convenient and are expensive. Most A-D-A type molecules still suffer from complex synthetic procedures, low overall yields and thus high costs.[48-50] To expand the diversity of A-D-A type molecules, herein we attempted to synthesize novel non-fused azacyclic pyrazolin-5-one end groups (Figure 1b) to replace the common end-group ICs and then connected them to the di-thienothiophen[3.2-*b*]-pyrrolobenzothiadiazole (BTP) core unit by the Knoevenagel condensation reaction, resulting in the corresponding new A-D-A type molecules BTP-P, BTP-pCP and BTP-mCP. Compared with the common IC end groups, non-fused pyrazoline-5-ones not only feature shorter reaction steps, higher yields, widely available and cheap reactants, simple and environmentally friendly synthesis and purification steps but also have more easily chemically modifiable sites due to the non-fused structure. Therefore, an end-group chlorination strategy on the end-group 3-methyl-1-phenyl-2-pyrazolin-5-one (PMP) was carried out and the corresponding chlorinated end-group derivatives pClPMP and mClPMP were obtained. Then, UV-visible absorption, cyclic voltammetry (CV), X-ray diffraction (XRD) and space charge limited current (SCLC) tests were also carried out to predict the properties of the three A-D-A type molecules BTP-P, BTP-pCP and BTP-mCP. These results indicate that the rational design of novel end group has the potential to improve the photovoltaic performance of solar cells.[51-53]

2 Results and discussion

1-Aryl-3-methyl-pyrazolin-5-ones were chosen as the end groups because they could be easily synthesized from arylhydrazine hydrochlorides and ethyl acetoacetate in the

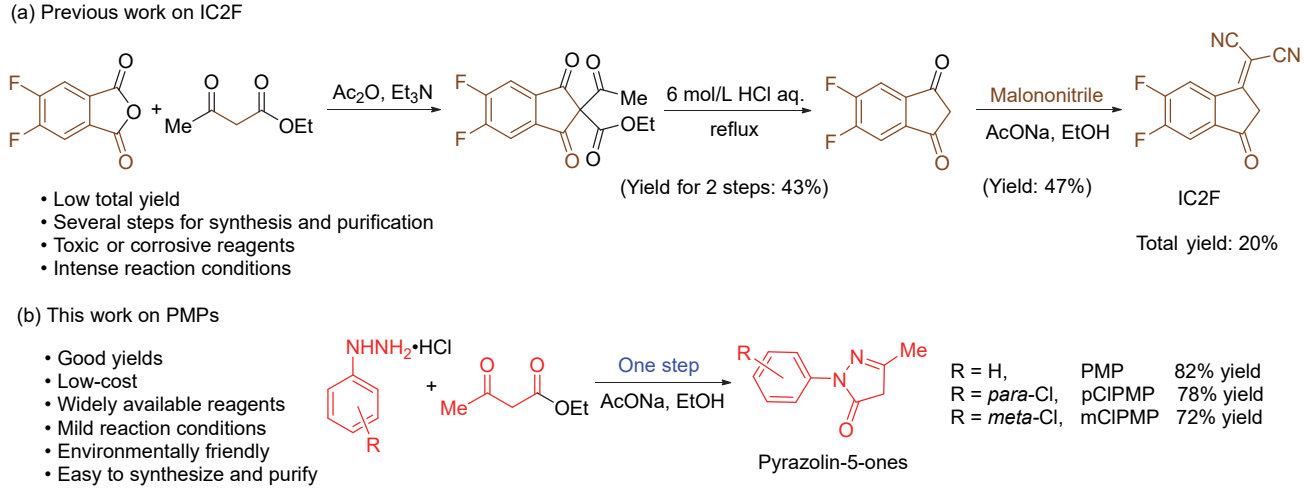

Figure 1 Structures and synthesis routes of IC2F in the previous work and PMPs in this work

presence of AcONa in EtOH at 75 °C for 12 h. Three representative 1-aryl-3-methyl-pyrazolin-5-ones including PMP (**2a**), also known as Edaravone or MCI-186, 1-(4-chlorophenyl)-3-methyl-2-pyrazolin-5-one (pClPMP, **2b**) and 1-(3-chlorophenyl)-3-methyl-2-pyrazolin-5-one (m-ClPMP, **2c**) were synthesized in one step and obtained in 72%～82% yields (Figure 2a). The synthesis of PMP, pCl-PMP and mClPMP only involved environmentally friendly reagents, that is, low-cost and widely available arylhydrazine hydrochlorides and ethyl acetoacetate. EtOH was used as the solvent, and AcONa acted as a base promoter. The reaction conditions were mild, and the products could be obtained in good yields and easily purified by recrystallization from absolute ethanol. Compared with the synthesis route of the end-group IC2F, the present protocol avoided the use of corrosive Ac_2O as the solvent and concentrated hydrochloric acid solution.

The cost of A-D-A type molecules is significant for fabricating solar cell devices. We attempted to calculate the material-only cost of end-group IC2F and PMP. Compared with the cost of approximately 76 dollars per gram of IC2F, the cost of PMP was no more than 3 dollars per gram, and the cost did not exceed 5 dollars per gram even for chlorine-substituted PMPs (Support Information, Tables S1～S4). In addition, we calculated the synthesis complexity (SC) to evaluate the synthesis route, yields and impacts on humans and the environment in the synthesis process (Support Information, Table S5).[54-55] SC was determined by the number of synthetic steps, the reciprocity yields, the number of unit operations, the number of column chromatography and the number of hazardous chemicals used for preparation by different weights. In the evaluation process, it was found that the values of the above five items in the synthesis of IC2F were higher than those in the synthesis of PMP. The SC value of PMP was determined to be only 33.0, assuming that the value of IC2F was 100 as the reference. The advantage of the low cost and smaller value of SC promoted our further research on PMPs.

The target molecules BTP-P (**3a**), BTP-pCP (**3b**) and BTP-mCP (**3c**) were synthesized by Knoevenagel condensation reaction of **1** with **2a**～**2c** assisted with pyridine at 65 °C for 32 h and were obtained in 61%～71% yields (Figure 2b). As shown in Figure 2, three molecules were constructed with a typical A-D-A structure and shared the same fused central core unit. Regulating the substituents of end-group PMPs helps to obtain structurally similar A-D-A type molecules. The obtained products have good solubility in solvents, such as chloroform and toluene, which are commonly used in the manufacturing process of solar cell devices.

To explore the stability and compositional uniformity of the designed A-D-A type molecules at the molecular level, theoretical calculations were conducted to determine the configuration and conformation of BTP-P and its derivatives (Figure 3). Quantum chemical calculations were per-

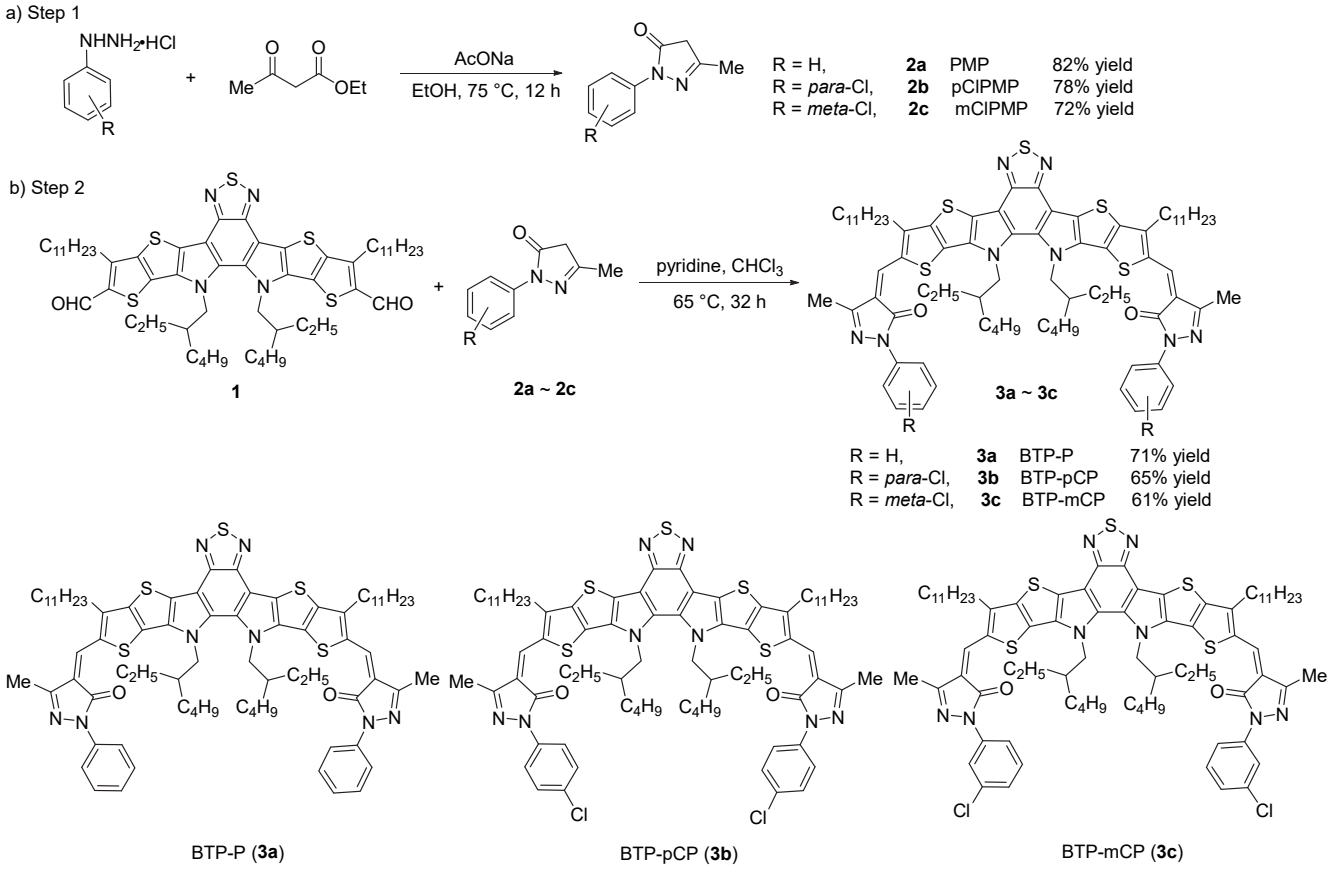

Figure 2 Synthetic route and molecular structures of BTP-P (**3a**), BTP-pCP (**3b**) and BTP-mCP (**3c**)

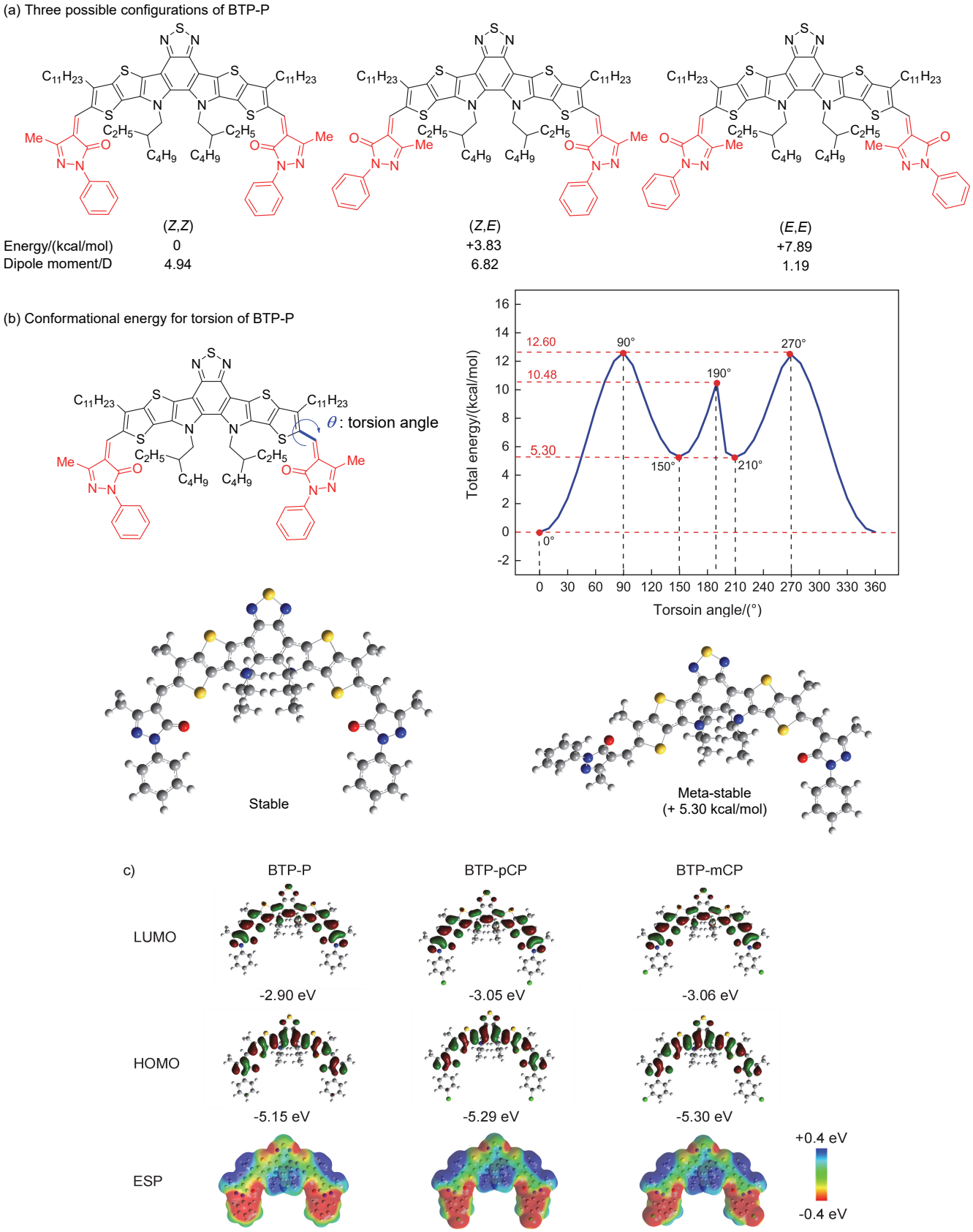

Figure 3 (a) Energies and dipole moments for three possible configurations of BTP-P calculated at the B3LYP/6-31G(d) level; (b) Torsion energies of BTP-P with torsion angles ranging from 0° to 360° (calculated at the B3LYP/6-31G(d) level); (c) Energy levels for the LUMO & HOMO and ESP diagrams of BTP-P, BTP-pCP and BTP-mCP

formed with density functional theory (DFT) at the B3LYP/6-31G(d) level using Gaussian 09 software. As shown in Figure 3, all three molecules **3a**～**3c** exhibited a planar conjugated framework structure, which facilitated π-π stacking and intermolecular charge transfer (ICT). Due to the asymmetry of the end-group PMP, the products generated through the Knoevenagel condensation reaction may have three possible configurations (*Z*,*Z*), (*Z*,*E*) and (*E*,*E*), as shown in Figure 3a. The relative energies of the three configurations of **3a** could be obtained by theoretical calculations. With the energy of the (*Z*,*Z*) configuration as the zero potential energy surface, the relative energies of the (*Z*,*E*) and (*E*,*E*) configurations of **3a** were 3.83 and 7.89 kcal/mol, respectively. Thus, the (*Z*,*Z*) configuration was the most stable and dominant one among the three configurations of BTP-P. The conformational energy of the most stable configuration was further investigated through theoretical calculations. A torsion energy scan on the single bond rotation at the end of the fused aromatic ring was performed (Figure 3b) and the dominant conformation was obtained. The torsion energy barrier $\Delta E_{torision}$ was 12.60 kcal/mol, which confirmed that planar BTP-P had a relatively stable configuration and conformation. This is crucial for end groups without large steric hindrance groups, which can avoid the high energy of recombination caused by configuration isomers and adverse conformational isomers caused by torsion conformations. Structural optimizations and frequency calculations for BTP-P, BTP-pCP and BTP-mCP were then conducted in order to predict the energies and orbital distributions of their highest occupied molecular orbitals (HOMOs) and lowest unoccupied molecular orbitals (LUMOs), and the energy differences and trends between the two orbitals were roughly estimated. According to Figure 3c, it could be inferred that the HOMOs and LUMOs of these molecules were mainly delocalized on the fused aromatic ring and pyrazolinones. The theoretically calculated HOMO/LUMO energy levels were −5.15 eV/−2.90 eV for BTP-P, −5.29 eV/−3.05 eV for BTP-pCP and −5.30 eV/−3.06 eV for BTP-mCP. A visualization of the electrostatic potential (ESP) is presented in Figure 3c. The effect of chlorine substitution on the charge distribution of A-D-A type molecules could be qualitatively illustrated. It is obvious that chlorine substitution enhances the electron deficiency of the PMP portion, and the position of chlorine substitution can regulate the charge distribution and polarity of the terminal portion.

The UV-vis absorption spectra of BTP-P, BTP-pCP and BTP-mCP in chloroform solution and solid films could reveal their optical properties and behaviours (Figure 4). In solution, the maximum absorption wavelengths (λ_{max}) of all these A-D-A type molecules were 620, 625 and 625 nm, respectively. Compared with absorption in solution, these molecules exhibited significant absorption redshifts in the films. The maximum absorption wavelengths of these molecules in the films were 655, 660 and 662 nm, respectively. The maximum absorption wavelengths of the three A-D-A type molecules were located between 550 nm for donors and 850 nm for molecules. Their absorption onsets were 713, 725 and 730 nm with corresponding optical gaps (ΔE_{opt}) of 1.74, 1.71 and 1.70 eV, respectively. It can be concluded that the electron-withdrawing effect of the end groups from PMP to pClPMP and mClPMP is enhanced, leading to an enhanced ICT effect, an absorption redshift, and a decrease in ΔE_{opt} (Figure 5b).

CV measurements were conducted on the films fabricated from the three A-D-A type molecules using ferrocene as the reference (Support Information, Figure S1), and the energy levels were obtained corresponding to their reduction and oxidation potential onsets, which were −5.42 eV/−3.62 eV for BTP-P, −5.43 eV/−3.68 eV for BTP-pCP and −5.43 eV/ −3.71 eV for BTP-mCP (Figure 5). These results indicated that the energy levels measured from CV agreed well with the trend of the predicted energy levels. The resulting electrochemical gaps ΔE_{CV} were 1.80, 1.75 and 1.72 eV, which were consistent with those derived from the UV-vis absorption measurements. Generally, these materials can adjust the interfacial properties of the active layer via effective and reasonable energy level arrangement, leading to the enhancement of short circuit current density (J_{SC}) and fill factor (FF). In the present case, the higher J_{SC} and FF expected to be observed in solar cell devices containing BTP-P or its derivatives could be attributed to a more ordered energy level cascade compared to the reference. Based on these optoelectronic properties, end-group engineering of the three A-D-A type molecules has shown potentials for regulating efficient

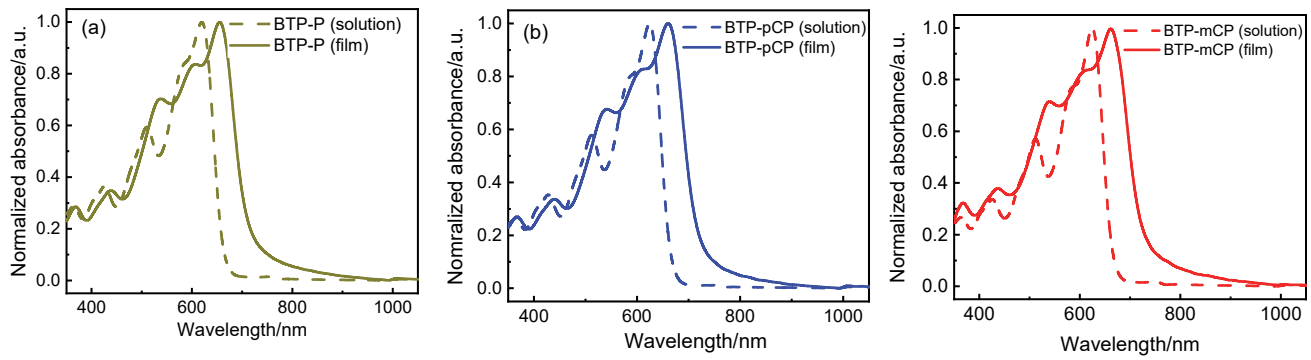

Figure 4 (a) UV-vis spectra of BTP-P in $CHCl_3$ solution and neat film; (b) UV-vis spectra of BTP-pCP in $CHCl_3$ solution and neat film; (c) UV-vis spectra of BTP-mCP in $CHCl_3$ solution and neat film

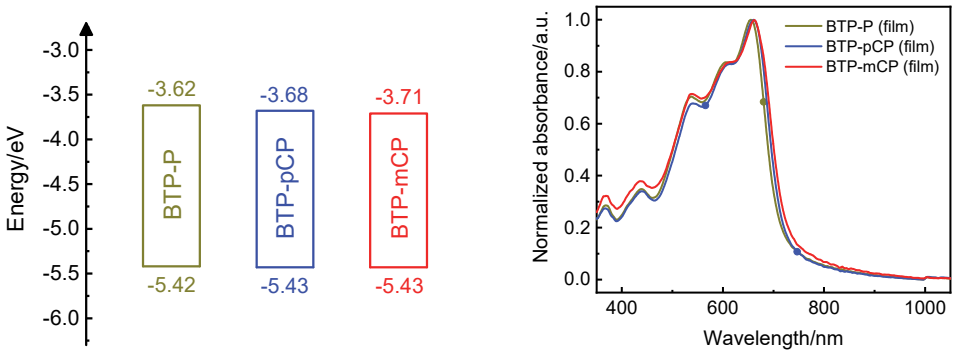

Figure 5 (a) HOMO/LUMO energy levels calculated from CV measurements; (b) UV-vis spectra of BTP-P, BTP-pCP and BTP-mCP in neat films.

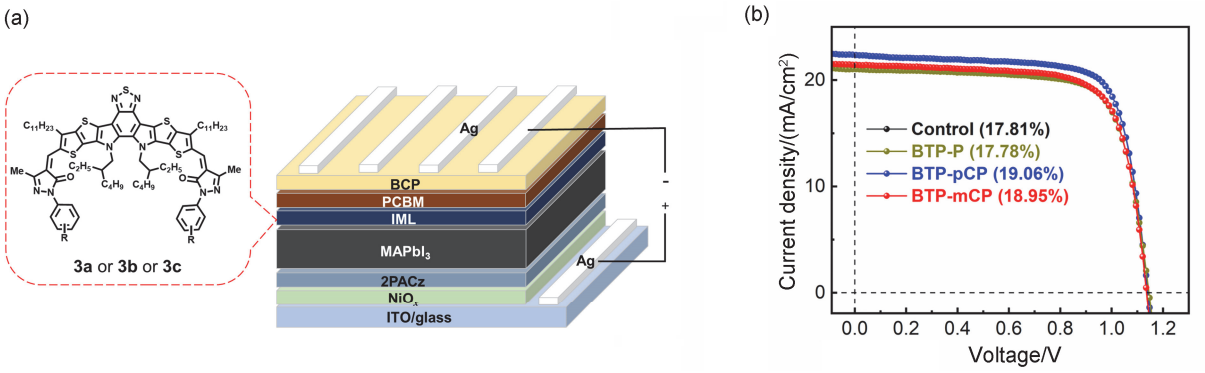

Figure 6 (a) Device structure; (b) *J-V* curves of best optimized devices with A-D-A type molecular interfacial modified layer and control devices

solar cells.

To further characterize the charge transfer properties of these A-D-A type molecules, the electron mobilities of BTP-P and its chlorinated derivatives in neat films were measured. The charge mobility was further evaluated by the SCLC method.[56,57] The electron mobility (μ_e) values of BTP-P and its chlorinated derivative neat films were 4.80×10^{-4}, 5.10×10^{-4} and 6.05×10^{-4} $cm^2\cdot V^{-1}\cdot s^{-1}$ for BTP-P, BTP-pCP and BTP-mCP, respectively (Support Information, Figure S2). The electron mobility results, as well as the UV-vis absorption and CV results mentioned above, indicated that BTP-P and its chlorinated derivatives had the potential to be applied to solar cell devices for interfacial modification of active layers.

To explore the impact of the molecular packing behaviours, XRD measurements for the neat films of BTP-P, BTP-pCP and BTP-mCP were performed (Support Information, Figure S3). According to Bragg's equation, it could be roughly estimated that the π-π stacking distances of the neat films fabricated with BTP-P, BTP-pCP and BTP-mCP were 3.50, 3.52 and 3.53 Å, respectively. The above results indicated that BTP-P shared similar π-π stacking modes after end-group regulation by chlorine substitution. It could be further inferred that the chlorine-substituted derivatives, compared to BTP-P, mainly changed the charge distribution and miscibility rather than the molecular packing distance.

In order to further verify the potential of the synthesized A-D-A type molecules (**3a**, **3b** and **3c**) for application in solar cells, we preliminarily applied them to perovskite solar cells as interfacial modified layer (IML).[58-60] The A-D-A type molecules were introduced as an ultra-thin interfacial modified layer to optimize the quality of the perovskite active layer by passivating surface, reducing defects and grain boundaries. As seen from the molecular structures of **3a**, **3b** and **3c** shown in Figure 2, it can be seen that PMP end groups contain Lewis-base functional groups including carbonyl and imine groups. These groups could potentially interreact with undercoordinated Pb^{2+} to form complexes.[59,61] In addition, the Cl atom in the end groups can further bind to excess Pb^{2+}.[62-63] Therefore, the introduction of the A-D-A type molecular interfacial modified layer has the potential to passivate surface defects and grain boundaries on the perovskite active layer to reduce carrier recombination and enhance performance.

The device structure is shown in Figure 6a, with ITO/NiO_x/2PACz/$MAPbI_3$/IML (**3a** or **3b** or **3c**)/PCBM/BCP/Ag from bottom to top, respectively. The device preparation procedures were described in details in the Support Information. The *J–V* curves of best optimized perovskite solar cells with A-D-A type molecular interfacial modified layer and control devices are presented in Figure 6b. These results showed that the interfacial modified layer had a significant effect on the efficiency performance of perov-

skite solar cells, causing obvious enhancement in fill factor.

Compared with the control devices, the perovskite solar cells with A-D-A type molecular interfacial modified layer demonstrated improved performance, and the detailed device parameters were shown in Table 1. The control devices showed the performance of V_{OC}, J_{SC}, FF and PCE in average, reaching 1.14 V, 21.28 mA•cm^{-2}, 71.96% and 17.39%, respectively. Meanwhile, the V_{OC}, J_{SC}, FF and PCE in average of perovskite solar cells with **3a** (BTP-P) as IML were 1.14 V, 20.82 mA•cm^{-2}, 74.07% and 17.57%, respectively. As a result, the average PCE of optimized devices showed that **3a** as IML had a quite limited positive enhancement effect. However, when **3b** or **3c** was applied as the IML of perovskite solar cells, it could be found that the A-D-A type molecules treated with end-group chlorination strategy as IML could help to achieve better performance of optimized devices. The V_{OC}, J_{SC}, FF and PCE in average of perovskite solar cells with **3b** (BTP-pCP) as IML were 1.13 V, 22.01 mA•cm^{-2}, 75.03% and 18.73%, respectively. In comparison, the V_{OC}, J_{SC}, FF and PCE in average of perovskite solar cells with **3c** (BTP-mCP) as IML were 1.13 V, 21.70 mA•cm^{-2}, 75.52% and 18.46%, respectively. Based on the above results, we attributed the promoting effect of **3b** and **3c** as the IML of the devices to the simultaneous enhancement of J_{SC} and FF.

3 Conclusion

In summary, three new A-D-A type molecules with a non-fused azacyclic pyrazolinones as the end groups were synthesized and applied as interfacial modified layer of the active layer in perovskite solar cells. By end-group engineering, BTP-P, BTP-pCP and BTP-mCP were synthesized through the Knoevenagel condensation reaction of the BTP core with a novel non-fused azacyclic end-group PMP, its *para*-chloro derivative or *meta*-chloro derivative, which were in turn prepared from low-cost, environmentally friendly and commercially available raw materials. DFT calculations were performed to predict the energy and molecular properties of these A-D-A type molecules. The optical and electrochemical properties of these materials were investigated to determine their optical gaps and HOMO/LUMO energy levels. Furthermore, UV-vis absorption, CV, XRD and SCLC characterizations were then conducted to verify the preliminary predictions of DFT calculations and explore the physiochemical properties of the A-D-A type molecules.

After investigating the properties of these A-D-A type molecules, their potential as interfacial modified layers in perovskite solar cell devices was further explored. It was found that the role of these A-D-A type molecules with non-fused azacyclic end groups as interfacial modified layers was mainly reflected in the increase of fill factor, compared to the reference device. Without chlorine substitution, its role as an interfacial modified layer was only to increase the fill factor, compromised by a slight decrease in J_{SC}. After the end-group chlorination modification, it not only increased the fill factor as an interfacial modified layer, but also increased the J_{SC}, ultimately resulting in an obvious improvement in PCE. These results demonstrate that the non-fused azacyclic A-D-A type molecules have the potentials to enhance the performance of solar cells and the end-group engineering is a promising strategy for fabricating high-performance devices.

4 Experimental section

4.1 Instruments and reagents

NMR spectra were recorded on a Bruker ASCEND III400 spectrometer at room temperature. ^{1}H NMR and ^{13}C NMR chemical shifts were determined relative to that of TMS. High resolution mass spectra (HRMS) were obtained on a Bruker UltrafleXtreme MALDI-TOF/TOF instrument. UV-vis spectra were obtained on a SHIMADZU UV-3600 PLUS. Cyclic voltammetry (CV) tests were conducted on a Shanghai Chenhua CHI630D workstation.

Reagents and solvents were commercially available and were used without any further purification. Compound **1** was synthesized according to the literature.[11]

4.2 General procedures for synthesis of compounds 2a～2c

A stirred solution of phenylhydrazine hydrochloride (10 mmol) dispersed in anhydrous ethanol (15 mL) was added with sodium acetate (11 mmol, 1.1 equiv) and ethyl acetoacetate (12 mmol, 1.2 equiv.). After the resulting reaction mixture was heated to 75 °C for 12 h, the mixture was cooled to −20 °C, and then the crude product was obtained

Table 1 Device parameters with BTP-P (**3a**), BTP-pCP (**3b**) and BTP-mCP (**3c**) as interface modification layer

Device		V_{OC}/V	J_{SC}/(mA•cm^{-2})	FF/%	PCE/%
Control	Average [a]	1.136±0.005	21.28±0.37	71.96±0.90	17.39±0.35
	Best	1.135	21.43	73.19	17.81
BTP-P treated	Average [a]	1.139±0.003	20.82±0.17	74.07±0.21	17.57±0.20
	Best	1.144	21.01	73.95	17.78
BTP-pCP treated	Average [a]	1.134±0.005	22.01±0.21	75.03±0.39	18.73±0.27
	Best	1.140	22.34	74.80	19.06
BTP-mCP treated	Average [a]	1.127±0.007	21.70±0.37	75.52±0.53	18.46±0.30
	Best	1.123	22.18	76.06	18.95

[a] The data were obtained from 5 independent devices.

by precipitation.[64] The crude product was purified by recrystallization in anhydrous ethanol to give compound **2**.

5-Methyl-2-phenyl-2,4-dihydro-3*H*-pyrazol-3-one (**2a**)[64]: Yellowish powder, yield 82%. ^{1}H NMR (400 MHz, $CDCl_3$) δ: 7.86 (d, J=7.7 Hz, 2H), 7.39 (dd, J=7.7, 7.4 Hz, 2H), 7.89 (t, J=7.4 Hz, 1H), 3.44 (s, 2H), 2.20 (s, 3H).

2-(4-Chlorophenyl)-5-methyl-2,4-dihydro-3*H*-pyrazol-3-one (**2b**)[64]: Yellowish powder, yield 78%. ^{1}H NMR (400 MHz, $CDCl_3$) δ: 7.85 (d, J=9.0 Hz, 2H), 7.35 (d, J=9.0 Hz, 2H), 3.44 (s, 2H), 2.21 (s, 3H).

2-(3-Chlorophenyl)-5-methyl-2,4-dihydro-3*H*-pyrazol-3-one (**2c**)[64]: Yellowish powder, yield 72%. ^{1}H NMR (400 MHz, $CDCl_3$) δ: 7.93 (t, J=2.0 Hz, 1H), 7.83 (ddd, J=8.2, 2.0, 0.9 Hz, 1H), 7.31 (t, J=8.1, Hz, 1H), 7.15 (ddd, J=8.1, 2.0, 0.9 Hz, 1H), 3.45 (s, 2H), 2.21 (s, 3H).

4.3 General procedures for synthesis of compounds 3a～3c

Compound **1** (0.02 mmol), compound **2** (0.20 mmol, 10 equiv) and pyridine (0.20 mmol, 10 equiv) were dissolved in chloroform (10 mL). The mixture was stirred at 65 °C for 32 h. After cooling to room temperature, the mixture was poured into methanol and filtered. The residue was purified by column chromatography on silica gel using ethyl acetate/petroleum ether (V∶V=1∶5) as the eluent to give the dark blue solid compound **3**.

(4*Z*,4'*Z*)-4,4'-((12,13-Bis(2-ethylhexyl)-3,9-diundecyl-12,13-dihydro[1,2,5]thiadiazolo[3,4-*e*]thieno[2",3":4',5']-thieno[2',3':4,5]pyrrolo[3,2-*g*]thieno[2',3':4,5]thieno[3,2-*b*]-indole-2,10-diyl)bis(methaneylylidene))bis(5-methyl-2-phenyl-2,4-dihydro-3*H*-pyrazol-3-one) (**3a**): Dark blue needle solid, yield 71%. ^{1}H NMR (400 MHz, $CDCl_3$) δ: 8.06 (d, J=7.6 Hz, 4H), 7.79 (s, 2H), 7.46 (dd, J=7.6, 7.4 Hz, 4H), 7.21 (t, J=7.4 Hz, 2H), 4.85～4.65 (m, 4H), 3.15 (t, J=7.6 Hz, 4H), 2.42 (s, 6H), 2.09 (t, J=6.0 Hz, 2H), 1.90 (t, J=7.2 Hz, 4H), 1.53～1.44 (m, 4H), 1.43～1.35 (m, 4H), 1.35～1.17 (m, 28H), 1.05～0.90 (m, 12H), 0.90～0.82 (m, 6H), 0.75～0.60 (m, 12H); ^{13}C NMR (101 MHz, $CDCl_3$) δ: 162.66, 149.99, 148.05, 147.57, 143.73, 138.66, 137.58, 133.42, 132.95, 132.87, 131.83, 128.81, 127.63, 124.62, 119.81, 118.97, 112.78, 55.48, 40.22, 31.89, 30.53, 29.69, 29.65, 29.60, 29.52, 29.41, 29.33, 29.14, 27.48, 27.43, 23.05, 23.02, 22.85, 22.68, 14.13, 13.70, 13.11, 10.21, 10.16; MALDI-TOF MS m/z calcd for $C_{78}H_{98}N_8O_2S_5$ $[M]^-$ 1338.6422, found 1338.6402.

(4*Z*,4'*Z*)-4,4'-((12,13-Bis(2-ethylhexyl)-3,9-diundecyl-12,13-dihydro[1,2,5]thiadiazolo[3,4-*e*]thieno[2",3":4',5']-thieno[2',3':4,5]pyrrolo[3,2-*g*]thieno[2',3':4,5]thieno[3,2-*b*]indole-2,10-diyl)bis(methaneylylidene))bis(2-(4-chlorophenyl)-5-methyl-2,4-dihydro-3*H*-pyrazol-3-one) (**3b**): Dark blue needle solid, yield 65%. ^{1}H NMR (400 MHz, $CDCl_3$) δ: 8.06 (d, J=8.9 Hz, 4H), 7.78 (s, 2H), 7.40 (d, J=8.9 Hz, 4H), 4.85～4.65 (m, 4H), 3.15 (t, J=7.5 Hz, 4H), 2.40 (s, 6H), 2.09 (t, J=5.9 Hz, 2H), 1.90 (t, J=7.2 Hz, 4H), 1.53～1.44 (m, 4H), 1.43～1.35 (m, 4H), 1.35～1.19 (m, 28H), 1.10～0.91 (m, 12H), 0.89～0.83 (m, 6H), 0.75～0.62 (m, 12H); ^{13}C NMR (101 MHz, $CDCl_3$) δ: 162.63, 150.32, 148.35, 147.55, 143.84, 137.51, 137.33, 133.67, 133.09, 133.04, 131.82, 129.52, 128.80, 127.94, 119.84, 119.43, 112.84, 55.51, 40.29, 31.89, 30.54, 29.70, 29.64, 29.60, 29.52, 29.41, 29.33, 29.16, 27.54, 27.48, 23.11, 23.07, 22.87, 22.68, 14.12, 13.73, 13.10, 10.23, 10.15; MALDI-TOF MS calcd for $C_{78}H_{96}Cl_2N_8O_2S_5$ 1406.5642, found 1406.5620.

(4*Z*,4'*Z*)-4,4'-((12,13-Bis(2-ethylhexyl)-3,9-diundecyl-12,13-dihydro[1,2,5]thiadiazolo[3,4-*e*]thieno[2",3":4',5']-thieno[2',3':4,5]pyrrolo[3,2-*g*]thieno[2',3':4,5]thieno[3,2-*b*]indole-2,10-diyl)bis(methaneylylidene))bis(2-(3-chlorophenyl)-5-methyl-2,4-dihydro-3*H*-pyrazol-3-one) (**3c**): Dark blue needle solid, yield 61%. ^{1}H NMR (400 MHz, $CDCl_3$) δ: 8.18 (s, 2H), 8.02 (dd, J=8.2 Hz, 1.2Hz, 2H), 7.79 (s, 2H), 7.38 (dd, J=8.2 Hz, 7.9 Hz, 2H), 7.17 (dd, J=7.9 Hz, 1.3 Hz, 2H), 4.85～4.69 (m, 4H), 3.16 (t, J=7.6 Hz, 4H), 2.42 (s, 6H), 2.08 (t, J=6.1 Hz, 2H), 1.91 (t, J=7.2 Hz, 4H), 1.53～1.45 (m, 4H), 1.44～1.36 (m, 4H), 1.35～1.19 (m, 28H), 1.09～0.90 (m, 12H), 0.89～0.84 (m, 6H), 0.74～0.60 (m, 12H); ^{13}C NMR (101 MHz, $CDCl_3$) δ: 162.76, 150.46, 148.39, 147.62, 143.84, 139.77, 137.47, 134.56, 133.73, 133.20, 133.12, 131.86, 129.82, 128.05, 124.39, 119.39, 118.59, 116.48, 112.80, 55.52, 40.32, 31.90, 30.55, 29.71, 29.65, 29.60, 29.52, 29.40, 29.33, 29.17, 27.62, 27.51, 23.12, 23.07, 22.87, 22.85, 22.68, 14.12, 13.77, 13.75, 13.12, 10.20, 10.10; MALDI-TOF MS calcd for $C_{78}H_{96}Cl_2N_8O_2S_5$ 1406.5642, found 1406.5617.

Supporting Information The details of experimental procedures, device fabrication, and NMR, MS and HPLC of the synthesized compounds. The Supporting Information is available free of charge via the Internet at http://sioc-journal.cn/.

References

[1] Yu, G.; Gao, J.; Hummelen, J. C.; Wudl, F.; Heeger, A. J. *Science* **1995**, *270*, 1789.

[2] Dou, L.; Liu, Y.; Hong, Z.; Li, G.; Yang, Y. *Chem. Rev.* **2015**, *115*, 12633.

[3] Yao, H.; Ye, L.; Zhang, H.; Li, S.; Zhang, S.; Hou, J. *Chem. Rev.* **2016**, *116*, 7397.

[4] Meng, L.; Zhang, Y.; Wan, X.; Li, C.; Zhang, X.; Wang, Y.; Ke, X.; Xiao, Z.; Ding, L.; Xia, R.; Yip, H.-L.; Cao, Y.; Chen, Y. *Science* **2018**, *361*, 1094.

[5] Cui, Y.; Xu, Y.; Yao, H.; Bi, P.; Hong, L.; Zhang, J.; Zu, Y.; Zhang, T.; Qin, J.; Ren, J.; Chen, Z.; He, C.; Hao, X.; Wei, Z.; Hou, J. *Adv. Mater.* **2021**, *33*, e2102420.

[6] Chong, K.; Xu, X.; Meng, H.; Xue, J.; Yu, L.; Ma, W.; Peng, Q. *Adv. Mater.* **2022**, *34*, e2109516.

[7] He, C.; Pan, Y.; Ouyang, Y.; Shen, Q.; Gao, Y.; Yan, K.; Fang, J.; Chen, Y.; Ma, C.-Q.; Min, J.; Zhang, C.; Zuo, L.; Chen, H. *Energy Environ. Sci.* **2022**, *15*, 2537.

[8] Zhang, G.; Lin, F. R.; Qi, F.; Heumüller, T.; Distler, A.; Egelhaaf, H.-J.; Li, N.; Chow, P. C. Y.; Brabec, C. J.; Jen, A. K.-Y.; Yip, H.-L. *Chem. Rev.* **2022**, *122*, 14180.

[9] Lin, Y.; Wang, J.; Zhang, Z. G.; Bai, H.; Li, Y.; Zhu, D.; Zhan, X. *Adv. Mater.* **2015**, *27*, 1170.

[10] Lin, Y.; Zhao, F.; Prasad, S. K. K.; Chen, J. D.; Cai, W.; Zhang, Q.;

Chen, K.; Wu, Y.; Ma, W.; Gao, F.; Tang, J. X.; Wang, C.; You, W.; Hodgkiss, J. M.; Zhan, X. *Adv. Mater.* **2018**, *30*, e1706363.
[11] Yuan, J.; Zhang, Y.; Zhou, L.; Zhang, G.; Yip, H.-L.; Lau, T.-K.; Lu, X.; Zhu, C.; Peng, H.; Johnson, P. A.; Leclerc, M.; Cao, Y.; Ulanski, J.; Li, Y.; Zou, Y. *Joule* **2019**, *3*, 1140.
[12] Cheng, P.; Li, G.; Zhan, X.; Yang, Y. *Nat. Photonics* **2018**, *12*, 131.
[13] Li, M.; Zhou, Y.; Zhang, J.; Song, J.; Bo, Z. *J. Mater. Chem. A* **2019**, *7*, 8889.
[14] Yan, C.; Barlow, S.; Wang, Z.; Yan, H.; Jen, A. K. Y.; Marder, S. R.; Zhan, X. *Nat. Rev. Mater*. **2018**, *3*, 18003.
[15] Zhu, L.; Zhang, M.; Xu, J.; Li, C.; Yan, J.; Zhou, G.; Zhong, W.; Hao, T.; Song, J.; Xue, X.; Zhou, Z.; Zeng, R.; Zhu, H.; Chen, C.-C.; MacKenzie, R. C. I.; Zou, Y.; Nelson, J.; Zhang, Y.; Sun, Y.; Liu, F. *Nat. Mater.* **2022**, *21*, 656.
[16] Zhang, C.; Song, J.; Ye, L.; Li, X.; Jee, M. H.; Woo, H. Y.; Sun, Y. *Angew. Chem. Int. Ed.* **2024**, *63*, e202316295.
[17] Li, X.; Luo, S.; Sun, H.; Sung, H. H.-Y.; Yu, H.; Liu, T.; Xiao, Y.; Bai, F.; Pan, M.; Lu, X.; Williams, I. D.; Guo, X.; Li, Y.; Yan, H. *Energy Environ. Sci*. **2021**, *14*, 4555.
[18] Jiang, K.; Wei, Q.; Lai, J. Y. L.; Peng, Z.; Kim, H. K.; Yuan, J.; Ye, L.; Ade, H.; Zou, Y.; Yan, H. *Joule* **2019**, *3*, 3020.
[19] Li, C.; Zhou, J.; Song, J.; Xu, J.; Zhang, H.; Zhang, X.; Guo, J.; Zhu, L.; Wei, D.; Han, G.; Min, J.; Zhang, Y.; Xie, Z.; Yi, Y.; Yan, H.; Gao, F.; Liu, F.; Sun, Y. *Nat. Energy* **2021**, *6*, 605.
[20] Qiao, Y.; Liu, X.; Li, Y.; Guo, X.; Li, C. *J. Mater. Chem. A* **2024**, *12*, 5493.
[21] Chen, Z.; Zhang, S.; Zhang, T.; Ren, J.; Dai, J.; Li, H.; Qiao, J.; Hao, X.; Hou, J. *Angew. Chem. Int. Ed*. **2024**, *63*, e202317892.
[22] Luo, D.; Zhang, L.; Zeng, J.; Chi, W.; Zhou, J.; Zhou, E.; Li, L.; Iwahashi, T.; Michinobu, T.; Ouchi, Y.; Xu, B.; Kyaw, A. K. K. *Adv. Funct. Mater.* **2024**, *34*, 2311736.
[23] Gao, Y.; Yang, X.; Sun, R.; Xu, L.-Y.; Chen, Z.; Zhang, M.; Zhu, H.; Min, J. *Joule* **2023**, *7*, 2845.
[24] Shi, S.; Zhang, S.; Yao, X.; Xian, K.; Han, D.; Zhu, Y.; Li, Y.; Tu, X.; Tang, Z.; Ye, L.; Zhong, H.; Fei, Z. *J. Mater. Chem. C* **2023**, *11*, 11943.
[25] Yang, Q.; Liu, X.; Yu, S.; Feng, Z.; Liang, L.; Qin, W.; Wang, Y.; Hu, X.; Chen, S.; Feng, Z.; Hou, G.; Wu, K.; Guo, X.; Li, C. *Energy Environ. Sci*. **2021**, *14*, 6536.
[26] Shi, Y.; Zhu, L.; Yan, Y.; Xie, M.; Liang, G.; Qiao, J.; Zhang, J.; Hao, X.; Lu, Kun; Wei, Z. *Adv. Energy Mater.* **2023**, *13*, 2300458.
[27] Yu, H.; Wang, Y.; Zou, X.; Han, H.; Kim, H. K.; Yao, Z.; Wang, Z.; Li, Y.; Ng, H. M.; Zhou, W.; Zhang, J.; Chen, S.; Lu, X.; Wong, K. S.; Zhu, Z.; Yan, H.; Hu, H. *Adv. Funct. Mater*. **2023**, *33*, 2300712.
[28] Li, H.; Li, J.; Yang, C.; Wang, J.; Ryu, D. H.; Ma, L.; Yang, Y.; Shin, W. S.; Zhang, S.; Hou, J. *J. Mater. Chem. C* **2023**, *11*, 6155.
[29] Luo, Z.; Yan, H.; Yang, C. *Acc. Mater. Res*. **2023**, *4*, 968.
[30] Pan, M.-A.; Lau, T.-K.; Tang, Y.; Wu, Y.-C.; Liu, T.; Li, K.; Chen, M.-C.; Lu, X.; Ma, W.; Zhan, C. *J. Mater. Chem. A* **2019**, *7*, 20713.
[31] An, Q.; Ma, X.; Gao, J.; Zhang, F. *Sci. Bull.* **2019**, *64*, 504.
[32] Li, K.; Wu, Y.; Tang, Y.; Pan, M.-A.; Ma, W.; Fu, H.; Zhan, C.; Yao, J. *Adv. Energy Mater.* **2019**, *9*, 1901728.
[33] Jiang, B.-H.; Chen, C.-P.; Liang, H.-T.; Jeng, R.-J.; Chien, W.-C.; Yu, Y.-Y. *Dyes Pigm*. **2020**, *181*, 108613.
[34] Elsayed, M. H.; Jiang, B.-H.; Wang, Y.-P.; Chang, P.-Y.; Chiu, Y.-C.; Jeng, R.-J.; Chou, H.-H.; Chen, C.-P. *J. Mater. Chem. A* **2021**, *9*, 9780.
[35] Fan, B.; Gao, W.; Wang, Y.; Zhong, W.; Lin, F.; Li, W. J.; Huang, F.; Yu, K.-M.; Jen, A. K. Y. *ACS Energy Lett.* **2021**, *6*, 3522.
[36] Li, Y.; Guo, Y.; Chen, Z.; Zhan, L.; He, C.; Bi, Z.; Yao, N.; Li, S.; Zhou, G.; Yi, Y.; Yang, Y.; Zhu, H.; Ma, W.; Gao, F.; Zhang, F.; Zuo, L.; Chen, H. *Energy Environ. Sci.* **2022**, *15*, 855.
[37] Ma, R.; Yan, C.; Yu, J.; Liu, T.; Liu, H.; Li, Y.; Chen, J.; Luo, Z.; Tang, B.; Lu, X.; Li, G.; Yan, H. *ACS Energy Lett.* **2022**, *7*, 2547.
[38] Murugan, P.; Hu, T.; Hu, X.; Chen, Y. *J. Mater. Chem. A* **2022**, *10*, 17968.
[39] Song, K. C.; Kim, B. J.; Sung, W.; Han, S. G.; Chung, S.; Lee, J.; Cho, K. *J. Mater. Chem. C* **2023**, *11*, 5354.
[40] Trippodo, E.; Campisciano, V.; Feng, L.-W.; Chen, Y.; Huang, W.; Alzola, J. M.; Zheng, D.; Sangwan, V. K.; Hersam, M. C.; Wasielewski, M. R.; Pignataro, B.; Giacalone, F.; Marks, T. J.; Facchetti, A. *J. Mater. Chem. C* **2023**, *11*, 8074.
[41] Han, C.; Wang, J.; Zhang, S.; Chen, L.; Bi, F.; Wang, J.; Yang, C.; Wang, P.; Li, Y.; Bao,X. *Adv. Mater*. **2023**, *35*, 2208986.
[42] Kim, K. S.; Chung, Y.; Praba, L.; Kim, D.; Park, J. B.; Jung, J. W. *Org. Electron.* **2024**, *125*, 106976.
[43] Pu, Z.; Li, J.; Xie, L.; Tong, X.; Yang, S.; Liu, J.; Chen, J.; Yang, M.; Yang, D.; Ge, Z. *Small* **2024**, *20*, 2310742.
[44] Liu, Z.; Lee, E. C. *Sustain. Energy Fuels* **2021**, *5*, 2354.
[45] Yang, G.; Afraj, S. N.; Li, J.; Zhang, D.; Fan, P.; Chen, M. C.; Zheng, D.; Yu, J. *J. Mater. Chem. C* **2024**, *12*, 3482.
[46] Song, C.; Li, X.; Wang, Y.; Fu, S.; Wan, L.; Liu, S.; Zhang, W.; Song, W.; Fang, J. *J. Mater. Chem. A* **2019**, *7*, 19881.
[47] Kuklin, S. A.; Safronov, S. V.; Fedorovskii, O. Y.; Khakina, E. A.; Peregudov, A. S.; Ezernitskaya, M. G.; Komissarova, E. A.; Emelianov, N. A.; Uvarov, M. N.; Kulik, L. V.; Frolova, L. A.; Troshin, P. A.; Khokhlov, A. R. *Org. Electron.* **2024**, *125s1*, 106978.
[48] Min, J.; Luponosov, Y. N.; Cui, C.; Kan, B.; Chen, H.; Wan, X.; Chen, Y.; Ponomarenko, S. A.; Li, Y.; Brabec, C. J. *Adv. Energy Mater.* **2017**, *7*, 1700465.
[49] Zhang, G.; Zhao, J.; Chow, P. C. Y.; Jiang, K.; Zhang, J.; Zhu, Z.; Zhang, J.; Huang, F.; Yan, H. *Chem. Rev.* **2018**, *118*, 3447.
[50] Li, X.; Pan, F.; Sun, C.; Zhang, M.; Wang, Z.; Du, J.; Wang, J.; Xiao, M.; Xue, L.; Zhang, Z. G.; Zhang, C.; Liu, F.; Li, Y. *Nat. Commun*. **2019**, *10*, 519.
[51] Shi, S.; Zhang, S.; Xue, Z.; Yao, X.; Zhang, J.; Gao, J.; Li, Y.; Tu, X.; Zhang, S.; Zhang, C.; Liu, Z.; Tang, Z.; Zhong, H.; Li, W.; Fei, Z. *ACS Appl. Mater. Interfaces* **2023**, *15*, 12119.
[52] Wang, H.; Zhang, C.; Yao, Y.; Cheng, C.; Wang, K. *Small* **2024**, 2403193.
[53] Wadsworth, A.; Bristow, H.; Hamid, Z.; Babics, M.; Gasparini, N.; Boyle, C. W.; Zhang, W.; Dong, Y.; Thorley, K. J.; Neophytou, M.; Ashraf, R. S.; Durrant, J. R.; Baran, D.; McCulloch, I. *Adv. Funct. Mater.* **2019**, *29*, 1808429.
[54] Yang, W.; Wang, W.; Wang, Y.; Sun, R.; Guo, J.; Li, H.; Shi, M.; Guo, J.; Wu, Y.; Wang, T.; Lu, G.; Brabec, C. J.; Li, Y.; Min, J. *Joule* **2021**, *5*, 1209.
[55] Luo, D.; Brabec, C. J.; Kyaw, A. K. K. *Nano Energy* **2023**, *114*, 108661.
[56] Cui, Y.; Yao, H.; Zhang, J.; Xian, K.; Zhang, T.; Hong, L.; Wang, Y.; Xu, Y.; Ma, K.; An, C.; He, C.; Wei, Z.; Gao, F.; Hou, J. *Adv. Mater.* **2020**, *32*, 1908205.
[57] Lin, F.; Jiang, K.; Kaminsky, W.; Zhu, Z.; Jen, A. K.-Y. *J. Am. Chem. Soc*. **2020**, *142*, 15246.
[58] Zheng, L.; Mukherjee, S.; Wang, K.; Hay, M. E.; Boudouris, B. W.; Gong, X. *J. Mater. Chem. A* **2017**, *5*, 23831.
[59] Lü, J.; Huo, X.; Liu, W.; Sun, W.; Ji, S.; You, T.; Wang, K.; Lü, W.; Wang, S. *Mater. Today Energy* **2024,** *44*, 101628.
[60] Afraj, S. N.; Velusamy, A.; Chen, C.-Y.; Ni, J.-S.; Ezhumalai, Y.; Pan, C.-H.; Chen, K.-Y.; Yau, S.-L.; Liu, C.-L.; Chiang, C.-H.; Wu, C.-G.; Chen, M.-C. *J. Mater. Chem. A* **2022**, *10*, 11254.
[61] Wang, D.; Ye, T.; Zhang, Y. *J. Mater. Chem. A* **2020**, *8*, 20819.
[62] Tavakoli, M. M.; Yadav, P.; Prochowicz, D.; Sponseller, M.; Osherov, A.; Bulovic´, V.; Kong, J. *Adv. Energy Mater*. **2019**, *9*, 201803587.
[63] Zhou, T.; Wang, K.; Zhu, D. ; Kuang, A. *J. Phys. Chem. Lett*. **2022**, *13*, 6074.
[64] Zhu, Y.-F.; Wei, B.-L.; Wei, J.-J.; Wang, W.-Q.; Song, W.-B.; Xuan, L.-J. *Tetrahedron Lett.* **2019**, *60*, 1202.

(Li, L.)

